

REPORT DOCUMENTATION PAGE			Form Approved OMB NO. 0704-0188		
<p>The public reporting burden for this collection of information is estimated to average 1 hour per response, including the time for reviewing instructions, searching existing data sources, gathering and maintaining the data needed, and completing and reviewing the collection of information. Send comments regarding this burden estimate or any other aspect of this collection of information, including suggestions for reducing this burden, to Washington Headquarters Services, Directorate for Information Operations and Reports, 1215 Jefferson Davis Highway, Suite 1204, Arlington VA, 22202-4302. Respondents should be aware that notwithstanding any other provision of law, no person shall be subject to any penalty for failing to comply with a collection of information if it does not display a currently valid OMB control number.</p> <p>PLEASE DO NOT RETURN YOUR FORM TO THE ABOVE ADDRESS.</p>					
1. REPORT DATE (DD-MM-YYYY) 21-09-2015		2. REPORT TYPE MS Thesis		3. DATES COVERED (From - To) -	
4. TITLE AND SUBTITLE Exfoliation and Stability Studies of Germanane and its Derivative (an Undergraduate Thesis)			5a. CONTRACT NUMBER W911NF-12-1-0481		
			5b. GRANT NUMBER		
			5c. PROGRAM ELEMENT NUMBER 611102		
6. AUTHORS Fan Fan, Joshua Goldberger (Advisor)			5d. PROJECT NUMBER		
			5e. TASK NUMBER		
			5f. WORK UNIT NUMBER		
7. PERFORMING ORGANIZATION NAMES AND ADDRESSES Ohio State University 1960 Kenny Road Columbus, OH 43210 -1016			8. PERFORMING ORGANIZATION REPORT NUMBER		
9. SPONSORING/MONITORING AGENCY NAME(S) AND ADDRESS (ES) U.S. Army Research Office P.O. Box 12211 Research Triangle Park, NC 27709-2211			10. SPONSOR/MONITOR'S ACRONYM(S) ARO		
			11. SPONSOR/MONITOR'S REPORT NUMBER(S) 62249-MS.13		
12. DISTRIBUTION AVAILABILITY STATEMENT Approved for public release; distribution is unlimited.					
13. SUPPLEMENTARY NOTES The views, opinions and/or findings contained in this report are those of the author(s) and should not be construed as an official Department of the Army position, policy or decision, unless so designated by other documentation.					
14. ABSTRACT The discovery of graphene has demonstrated that stable single-layer sheets can be isolated from the bulk materials. In the previous work, we have successfully isolated single-layer hydrogen-terminated-germanium (germanane, GeH) sheets which have unique electronic properties distinct from the bulk materials and can be applied on several areas such as sensors and transparent conducting electrodes. In order to improve the conductivity of GeH, we have synthesized phosphorus-doped germanane (P-GeH), gallium-doped germanane (Ga-GeH) and					
15. SUBJECT TERMS 2D Materials beyond Graphene, Graphane, Germanane					
16. SECURITY CLASSIFICATION OF:			17. LIMITATION OF ABSTRACT UU	15. NUMBER OF PAGES	19a. NAME OF RESPONSIBLE PERSON Joshua Goldberger
a. REPORT UU	b. ABSTRACT UU	c. THIS PAGE UU			19b. TELEPHONE NUMBER 614-247-7438

Report Title

Exfoliation and Stability Studies of Germanane and its Derivative (an Undergraduate Thesis)

ABSTRACT

The discovery of graphene has demonstrated that stable single-layer sheets can be isolated from the bulk materials. In the previous work, we have successfully isolated single-layer hydrogen-terminated-germanium (germanane, GeH) sheets which have unique electronic properties distinct from the bulk materials and can be applied on several areas such as sensors and transparent conducting electrodes. In order to improve the conductivity of GeH, we have synthesized phosphorus-doped germanane (P-GeH), gallium-doped germanane (Ga-GeH) and arsenic-doped germanane (As-GeH) via the topochemical deintercalation of CaGeP, GaGeGa and CaGeAs, respectively. Similar to GeH, the doped GeH can also be exfoliated into single- and few-layer sheets on SiO₂/Si substrates mechanically. The suggested tape for exfoliating the four materials as measurable multilayer flakes is polydimethylsiloxane (PDMS) and lithium phenylacetylide can remove the PDMS residues on the exfoliated flakes. All the four van der Waals materials can be oxidized in the air with different oxidizing rates but the oxidation is limited to the surface layers based on the X-ray photoelectron spectroscopy and atomic force microscopy (AFM). In addition, the oxidized layers can dissolve in the HCl aqueous solution but the fresh layers are resistant to the HCl aqueous solution.

Exfoliation and Stability Studies of Germanane and its Derivatives

Research Thesis

Presented in Partial Fulfillment of the Requirements for graduation

“with Research Distinction in Chemistry” in the undergraduate colleges of The Ohio State
University

By

Fan Fan

The Ohio State University

November 2014

Thesis Committee:

Joshua Goldberger, Project Advisor

Yiying Wu

Abstract

The discovery of graphene has demonstrated that stable single-layer sheets can be isolated from the bulk materials. In the previous work, we have successfully isolated single-layer hydrogen-terminated-germanium (germanane, GeH) sheets which have unique electronic properties distinct from the bulk materials and can be applied on several areas such as sensors and transparent conducting electrodes. In order to improve the conductivity of GeH, we have synthesized phosphorus-doped germanane (P-GeH), gallium-doped germanane (Ga-GeH) and arsenic-doped germanane (As-GeH) via the topochemical deintercalation of CaGeP, GaGeGa and CaGeAs, respectively. Similar to GeH, the doped GeH can also be exfoliated into single- and few-layer sheets on SiO₂/Si substrates mechanically. The suggested tape for exfoliating the four materials as measurable multilayer flakes is polydimethylsiloxane (PDMS) and lithium phenylacetylide can remove the PDMS residues on the exfoliated flakes. All the four van der Waals materials can be oxidized in the air with different oxidizing rates but the oxidation is limited to the surface layers based on the X-ray photoelectron spectroscopy and atomic force microscopy (AFM). In addition, the oxidized layers can dissolve in the HCl aqueous solution but the fresh layers are resistant to the HCl aqueous solution.

Acknowledgments

First of all, I would express my sincerest gratitude to my thesis advisor, Prof. Joshua Goldberger and thank you so much for offering a research opportunity, constant support and patient guidance on my thesis. Thank you to Basant Chitara for your suggestions at the beginning of my thesis. I would also like to thank Nick Cultrara and Shishi Jiang for preparing awesome crystal samples and suggestions to my work. Finally, I would like to extend a special gratitude to my parents for their endless support in the past two and half years.

Vita

Education

2012.....Heilongjiang University, Heilongjiang Province, China
2014..... B.S., Chemistry with ASC certification

Field of Study

Major Field: Chemistry

Table of Contents

Abstract	i
Acknowledgements	ii
Vita	iii
List of Figures	v
Chapter 1: Introduction	1
Chapter 2: Optimized Exfoliation of Multilayers	
2.1: Exfoliation and Characterization	4
2.2: Optimized Tape Choice for Exfoliation	8
2.3: Optimized Cleaning Process	10
Chapter 3: Synthesis and Characterization of Germanane and its Derivatives	12
Chapter 4: Stability Studies	
4.1: Air-Stability (XPS)	15
4.2: Air-Stability (AFM)	17
4.3: HCl-Stability	20
Chapter 5: Further Work	22
Conclusion	24
References	25

List of Figures

Figure 2.1. Optical micrograph of SiO ₂ /Si wafer and applied substrate (right corner)	4
Figure 2.2. (a) AFM image (top), optical image (inset) and height profile of few-layer GeH flake on SiO ₂ /Si. (b) AFM image (top), optical image (inset) and height profile of single-atom-thick GeH flake	5
Figure 2.3. (a) AFM image (top), height profile (bottom), and optical micrograph (inset) of 9.85-nm-thick P-GeH sheet. (b) AFM image (top), height profile (bottom), and optical micrograph (inset) of 9.1-nm-thick P-GeH sheet	6
Figure 2.4. (a) AFM image (top), height profile (bottom), and optical micrograph (inset) of 14-nm-thick P-GeH sheet. (b) AFM image (top), height profile (bottom), and optical micrograph (inset) of 17.3-nm-thick P-GeH sheet	6
Figure 2.5. (a) AFM image (top), height profile (bottom), and optical micrograph (inset) of 23.6-nm-thick P-GeH sheet. (b) AFM image (top), height profile (bottom), and optical micrograph (inset) of 36.2-nm-thick Ga-GeH sheet	7
Figure 2.6. AFM image (top), height profile (bottom), and optical micrograph (inset) of 115.4-nm-thick GeH sheet	7
Figure 2.7. Diagrammatic sketch of atomic force microscopy (AFM) structure	8
Figure 2.8. (a) Optical image of scotch tape. (b) Optical image of polydimethylsiloxane (PDMS). (c) Optical image of Kapton tape	9
Figure 2.9. (a) Optical image of spin-coat comparison test sample. The left 4 substrates were exfoliated by the scotch tape while the right 4 were exfoliated by kapton tape. (b) AFM image (top), height profile (bottom), and optical micrograph (inset) of a scotch tape exfoliated As-GeH sample. (c) AFM image (top), height profile (bottom), and optical micrograph (inset) of a PDMS exfoliated Ga-GeH sample	10
Figure 2.10. (a) Fresh exfoliated Ga-GeH flake. (b) The same flake after 90 min lithium phenylacetylide treatment. (c) Height profile of (a) and (b)	11
Figure 2.11. Schematic illustration of PDMS dissolving in lithium phenylacetylide	11
Figure 3.1 (a) Schematic illustration of the GeH preparation. 9b) Optical image of CaGe ₂ crystal. (c) Optical image of GeH crystal. (d) XRD diagram of (b). (e) XRD diagram of GeH	12
Figure 3.2. Schematic diagrams of (a) Ga-GeH and (b) As-GeH and p-GeH	13
Figure 3.3. (a) XRD spectra (b) FTIR spectra and (c) Raman spectra of Ga-GeH, As-GeH and GeH	14
Figure 4.1. (a) 3d XPS spectra and (b) 2p XPS spectra of As-GeH	16
Figure 4.2. (a) 3d XPS spectra and (b) 2P XPS spectra of Ga-GeH	16

Figure 1.3. Time-dependent XPS spectra of GeH after exposure to the air for a period of time	17
Figure 4.4. (a) AFM image of a fresh Ga-GeH flake. (b) AFM image of (a) after one week in air. (c) AFM image of (b) after 30 seconds 1 M HCl treat. (d) Height profile of (a), (b) and (c). (e) AFM of another fresh Ga-GeH flake. (f) AFM of (e) after 30 seconds in 1 M HCl. (g) Height profile of (e) and (f)	17
Figure 4.5. (a) AFM image of a fresh As-GeH flake. (b) AFM image of (a) after one week in air. (c) Height profile of (a) and (b). (d) AFM of another fresh As-GeH flake. (e) AFM of (d) after 30 seconds in 1 M HCl. (f) Height profile of (d) and (e)	18
Figure 4.6. a) AFM image of a fresh P-GeH flake. (b) AFM image of (a) after one week in air. (c) Height profile of (a) and (b). (d) AFM of another fresh P-GeH flake. (e) AFM of (d) after 30 seconds in 1 M HCl. (f) Height profile of (d) and (e)	19
Figure 4.7. a) AFM image of a fresh GeH flake. (b) AFM image of (a) after one week in air. (c) Height profile of (a) and (b). (d) AFM of another fresh GeH flake. (e) AFM of (d) after 30 seconds in 1 M HCl. (f) Height profile of (d) and (e)	19
Figure 4.8. (a) AFM image of fresh-exfoliated Ga-GeH. (b) AFM image of (a) after 30 seconds 1 M HCl treatment. (c) AFM image of (b) after 1200 seconds 1 M HCl treatment. (d) Height profile of (a), (b) and (c)	20
Figure 5. (a) AFM image of fresh Ga-GeH flake. (b) AFM of (a) after 30 second oxygen plasma followed by 30 seconds 1 M HCl treatment. (c) Height profile of (a) and (b). (d) AFM of fresh Ga-GeH flake. (e) AFM of (d) after 30 seconds UV-ozone plasma followed by 30 seconds 1 M HCl. (f) Height profile of (d) and (e)	23

Chapter 1: Introduction

The discovery of stable single-atom-thick graphene has also demonstrated that it is possible to isolate stable single-layer-thick materials from the bulk materials whose crystal structures are mainly bonded by weak van der Waals interactions.¹ The isolated single-layer materials have unique electric properties distinct from their parent materials which make them promising candidates in potential applications such as sensors, transistors and transparent conducting electrodes.²⁻⁵ Graphene's success motivates the exploration of the properties and stability of other single-layer 2D materials. For example, MoS₂ crystals have a 1.29 eV indirect band gap while its single-layer sheets have a direct band gap at 1.8 eV which reveals the potential application as high mobility transistors for isolated MoS₂ single layers.⁶⁻⁸

As for 2D materials, their binding strength on the 2D direction is much stronger than it of a third dimension. It has been demonstrated that most semiconductor material crystals from II-VI groups can be dimensionally reduced to 2D materials under solution-phase solvothermal synthesis method accompanying with alkylamine ligands.⁹⁻¹³ The conventional van der Waals materials are not chemical functionalized which limits the practical applications. In contrast, the 2D materials would have a wide of optical and electronic applications after adding electrically active layers. This terminal substituent creates a new direction to not only modify the fundamental electric properties of layered materials but also functionalize the layered materials based on the specific sensing applications. For example, graphene have been reported to be grafted with some organic functional groups, terminated with hydrogen and be oxidized.^{14,15} However, the original mobility of carriers is undermined for the functionalized layer materials and the stability is also eliminated.¹⁶

It has been demonstrated that the GaGe_2 can be converted to the hydrogen-terminated germanium crystals in concentrated HCl aqueous solution.¹² The Ge in GeH crystals is in the sp^3 -hybridized state which may maintain good conductivity. Recently, Goldberger's group has developed gram-scale crystallites of GeH whose single-layer sheet has a calculated 1.53 eV direct band gap and has proven that the GeH surface layers would be oxidized slowly in the air.¹³ In order to make hydrogen-terminated germanium more applicable, we want to develop both n-doping and p-doping germanane crystals to tune the optical and electric properties of GeH for practical applications.¹⁷

The apparent and useful electric properties such the direct band gap is based on the single-layer sheets. Generally, the weak van der Waals interactions between two adjacent sheets are just 40 meV to ~ 70 meV so single-layer sheets and multilayer sheets can be collected by exfoliation. Mechanical exfoliation which uses tapes such as scotch tape to isolate thin sheets is the most common and powerful exfoliation method because this method does not destroy thin flakes easily compared with other methods including chemical exfoliation and can create large single-atom-thick flakes ($\sim 10\mu\text{m}$ level) which is convenient for making fabricating devices.¹⁷ We have demonstrated that the pure GeH has being exfoliated into single layer sheets at $2\mu\text{m} \times 2\mu\text{m}$ level.¹⁸

In order to modify the resistance of GeH for practical applications, we successfully synthesis three doped GeH: P-GeH, Ga-GeH and A-GeH. In addition, we exfoliate the three types of doped GeH into multilayers with measureable size ($> 5\mu\text{m} \times 5\mu\text{m}$) onto SiO_2/Si substrates. The Polydimethylsiloxane (PDMS) is the optimized tape for exfoliation while lithium phenylacetylide is added to optimize the cleaning effect. Besides, we prove by XPS and AFM measurements that all four types of GeH would be oxidized for one week exposure in the air

when exfoliated as multilayer sheets. The oxidizing rates would vary but the oxidization is limited on the surface layers. The oxidized parts can be dissolved by HCl aqueous solution while the fresh parts are resistant to HCl aqueous solution. Finally, we start performing four-probe and three-probe measurements to study the pure resistance of GeH materials, the carrier-concentration-dependent conductivity, the mobility of carriers and the identify the carriers.

Chapter 2: Optimized Exfoliation of Multilayers

2.1 Exfoliation and Characterization

GeH is a van der Waals material and its crystal structure consists of single GeH sheets held mainly by weak van der Waals interactions. Therefore, single- and multi-atom-thick GeH layers can be isolated from the bulk materials via the mechanical exfoliation which has been demonstrated.¹² Similarly, three doped GeH share the same interlayer interactions with pure GeH and can be exfoliated into single layers and multilayers on SiO₂/Si substrates (**Figure 2.1**). Generally, 1cm×1cm SiO₂/Si substrates would be sonicated before exfoliation in acetone and isopropanol for 20 minutes, respectively, rinsed by deionized water and followed by 5-minute oxygen plasma treatment. The pre-exfoliation cleaning process is expected to remove both chemical residues and physical junks in order to create a clean and flat surface for getting flat exfoliated flakes. After exfoliation, the exfoliated samples are soaked in acetone and isopropanol

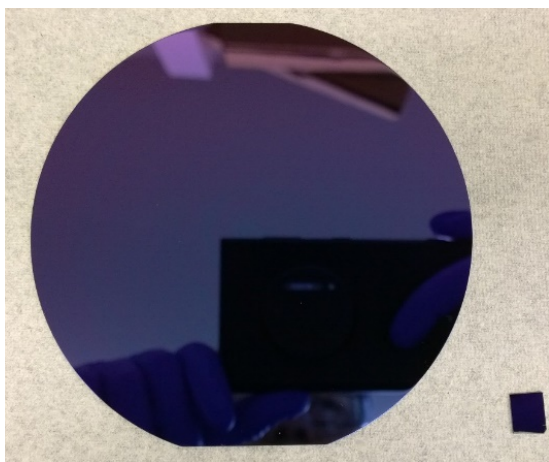


Figure 2.1. Optical micrograph of SiO₂/Si wafer and applied substrate (right corner).

for one hour, respectively, followed by deionized water rinsing and nitrogen flow drying.

The exfoliated flakes would be located via a microscope and evaluated by the atomic force microscopy (AFM). The combination of optical micrographs and AFM micrographs proves that the color of exfoliated thin sheets is related to its thickness. The previous work showed that

single-layer sheets are violet under the microscope (**Figure 2.2**).¹³ When the thickness of exfoliated sheets is lower than 10 nm, their color becomes deep blue (**Figure 2.3**). The optical color would be blue/cyan if the thickness range is from 13 nm to 27 nm (**Figure 2.4, 2.5a**). As the thickness of thin sheets continues to increase (< 45 nm), the optical color would turn to green/yellow (**Figure 2.5b**). In addition, the optical micrograph of thin sheets also become more massive with increasing thickness and the uniformity of surface color means a flat surface (**Figure 2.5, 2.6**). Atomic force microscopy (AFM) is a precise probe for analyzing the surface at nanoscale and its images (**Figure 2.2 – 2.6**) can evaluate the exfoliated flakes quantitatively to see if they are capable of making fabricating devices. Generally, the AFM probe (**Figure 2.7**) is oscillated at its fundamental resonance and the oscillation amplitude (the detector signal) can be

set to keep a constant distance between the probe and the analyzed surface so the output single offers the thickness information of particles on the scanned surface.

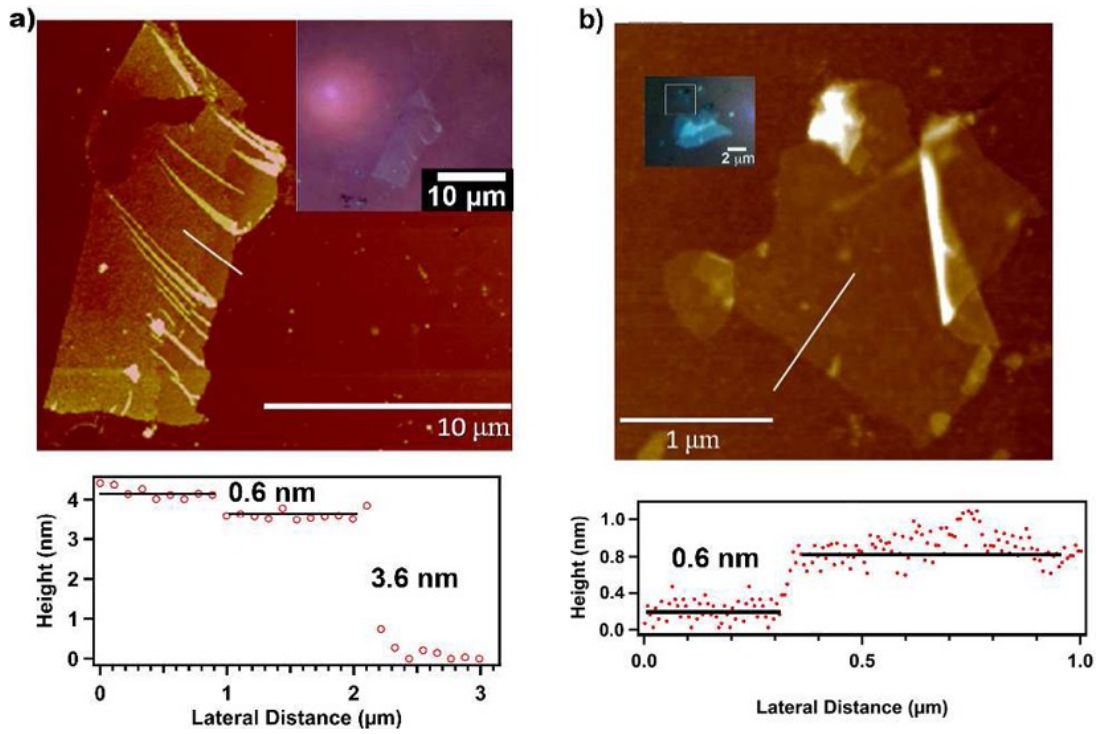


Figure 2.2. (a) AFM image (top), optical image (inset) and height profile of few-layer GeH flake on SiO_2/Si . (b) AFM image (top), optical image (inset) and height profile of single-atom-thick GeH flake.¹⁸

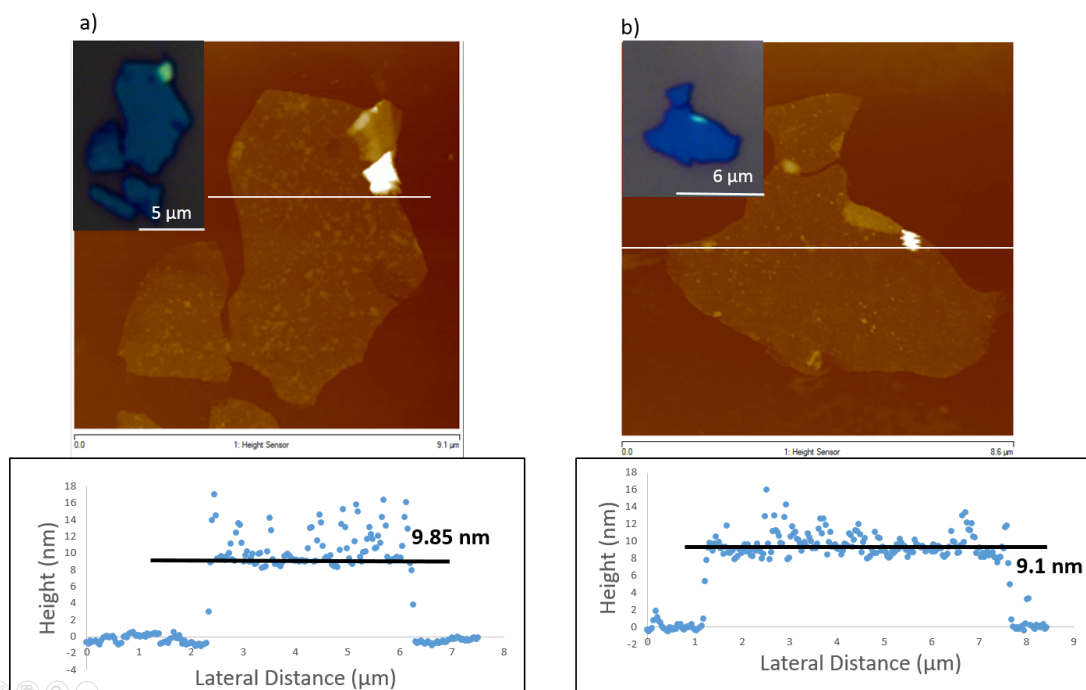


Figure 2.3. (a) AFM image (top), height profile (bottom), and optical micrograph (inset) of 9.85-nm-thick P-GeH sheet. (b) AFM image (top), height profile (bottom), and optical micrograph (inset) of 9.1-nm-thick P-GeH sheet.

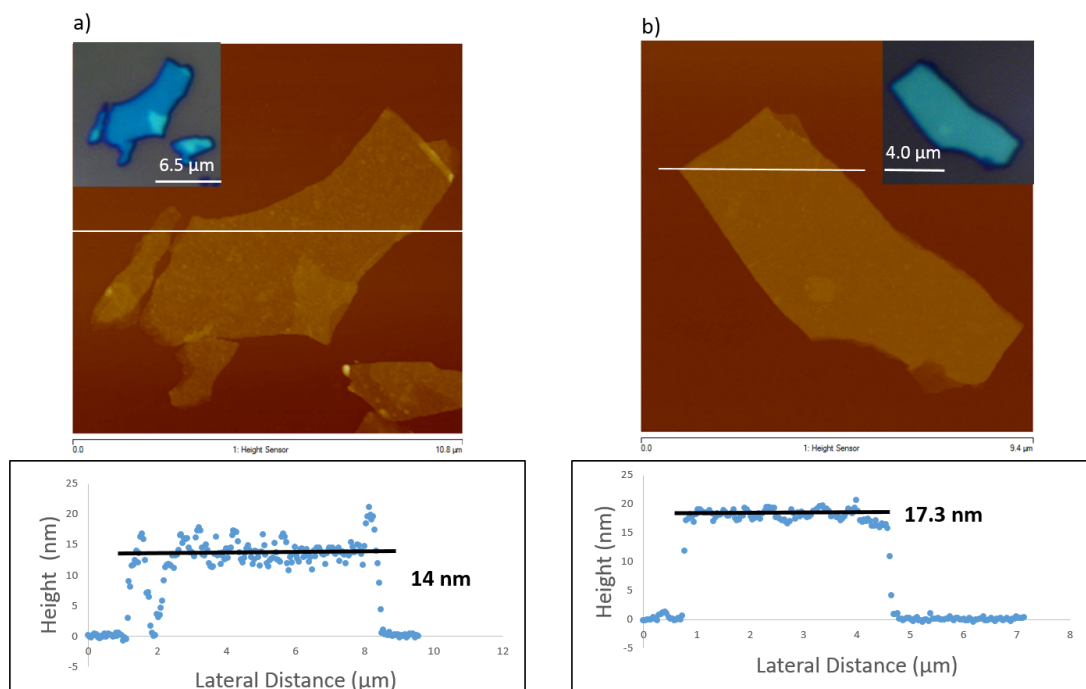


Figure 2.4. (a) AFM image (top), height profile (bottom), and optical micrograph (inset) of 14-nm-thick P-GeH sheet. (b) AFM image (top), height profile (bottom), and optical micrograph (inset) of 17.3-nm-thick P-GeH sheet.

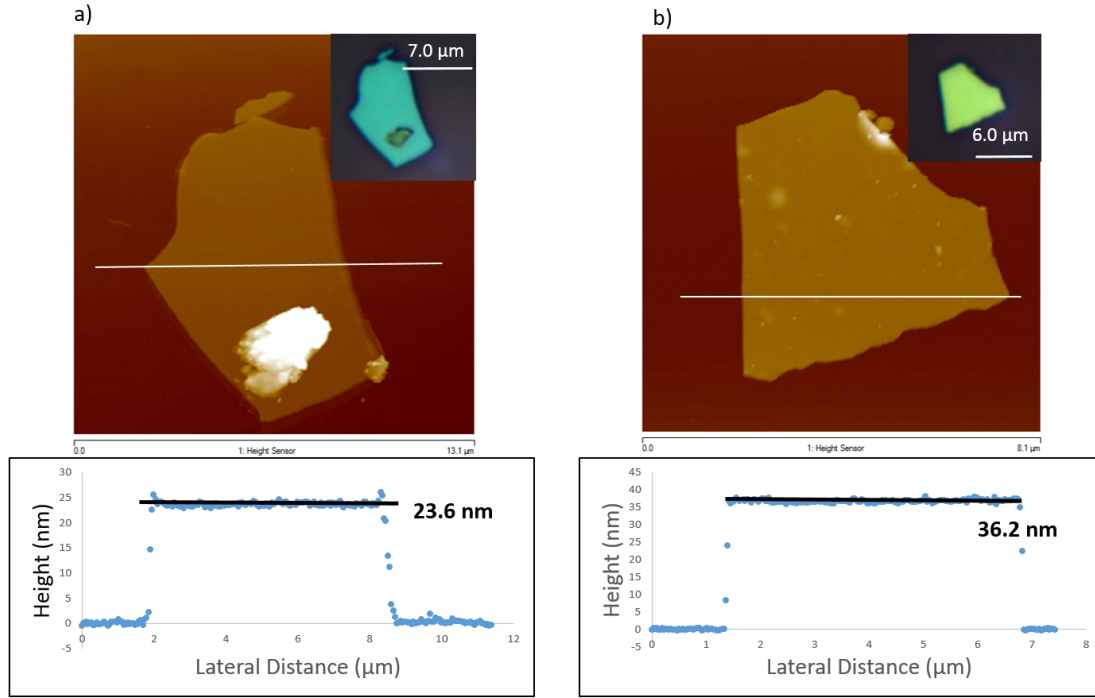


Figure 2.5. (a) AFM image (top), height profile (bottom), and optical micrograph (inset) of 23.6-nm-thick P-GeH sheet. (b) AFM image (top), height profile (bottom), and optical micrograph (inset) of 36.2-nm-thick Ga-GeH sheet.

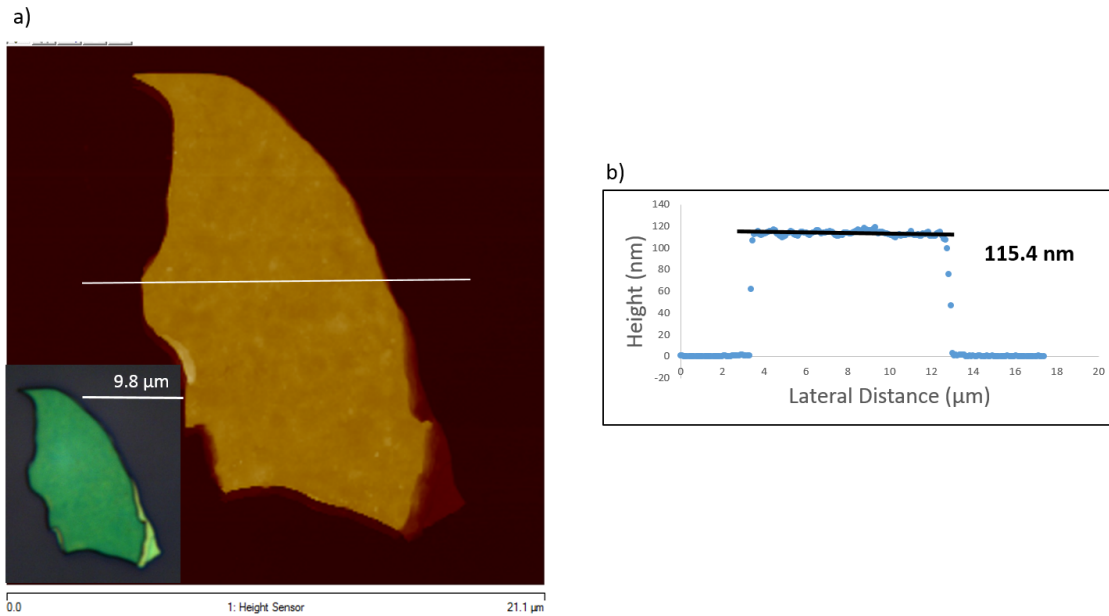


Figure 2.6. AFM image (top), height profile (bottom), and optical micrograph (inset) of 115.4-nm-thick GeH sheet.

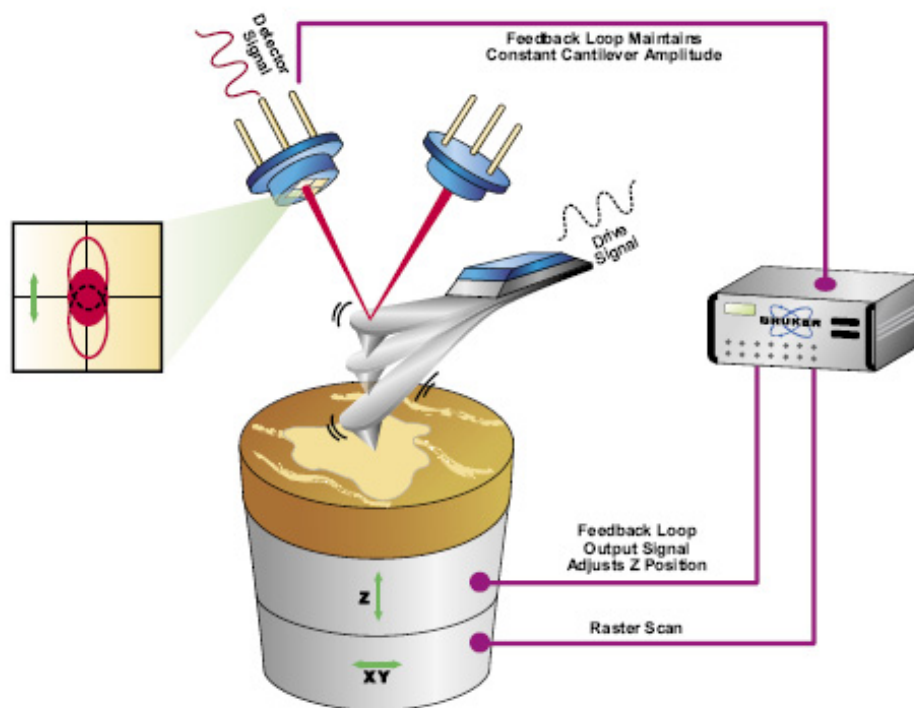


Figure 2.7. Diagrammatic sketch of atomic force microscopy (AFM) structure.

2.2 Optimized Tape Choice for Exfoliation

As for exfoliation, choosing a suitable tape is important. Exfoliated flakes would finally be used to make fabricating devices for the further studies on optical and electronic properties. When preparing fabricating devices, flakes would be spin-coated with methyl methacrylate (MMA) first followed by poly (methyl methacrylate) (PMMA). After baking the spin-coated substrates for a period of time, the electron beam operation (E-beam) would be placed on the MMA-PMMA-covered surface in order to remove the residues on the thin sheets. Methyl isobutyl ketone (MIBK) and isopropanol are applied on the substrate surface as the developer to adhere the metal conductors. Finally, the fabricating device would be rinsed by acetone to remove MMA and PMMA. In order to characterize the electric properties, four-probe and three-probe measurements would be placed on the fabricating devices so the acceptable thin flakes

should be at least $5\text{ }\mu\text{m} \times 5\text{ }\mu\text{m}$. A flat surface is also required or the metal conductors cannot touch the flakes well which can disrupt the electric property studies. The ideal thickness of an exfoliated sheet is $\sim 5.5\text{ }\text{\AA}$ which is a single layer sheet because the calculated 1.53 eV direct band gap is for the single-atom-thick GeH sheets but not the bulk GeH crystals.¹³

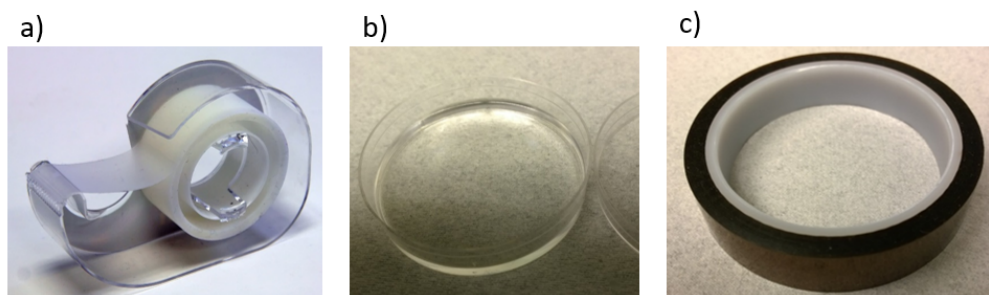


Figure 2.8. (a) Optical image of scotch tape. (b) Optical image of polydimethylsiloxane (PDMS). (c) Optical image of Kapton tape.

We used scotch tape (**Figure 2.8a**), polydimethylsiloxane (PDMS) (**Figure 2.8b**), and kapton tape (**Figure 2.8c**) to exfoliate four types of GeH crystals onto the SiO_2/Si substrates. Kapton tape can produce flat and large enough flakes for fabricating devices (**Figure 2.5a**). However, the kapton-tape-exfoliated samples cannot be spin-coated uniformly because of the tape residues left on the surface and these residues can block the spin-coat process (**Figure 2.9a right**). In contrast, the scotch-tape-exfoliated samples can be spin-coated uniformly (**Figure 2.9a left**) although the exfoliated flakes are not flat and the surface is covered by residues (**Figure 2.9b**). In previous work, the single-layer GeH sheet was firstly exfoliated by PDMS which is made by mixing silicone elastomer base and silicone elastomer curing agent together by the mass ratio of 10:1. Distinct from previous two tapes, PDMS is slightly sticky but very clean without aging disruption and flakes exfoliated by PDMS are flat and measurable (**Figure 2.9c**). Therefore, PDMS is the optimized tape choice among tapes we have investigated.

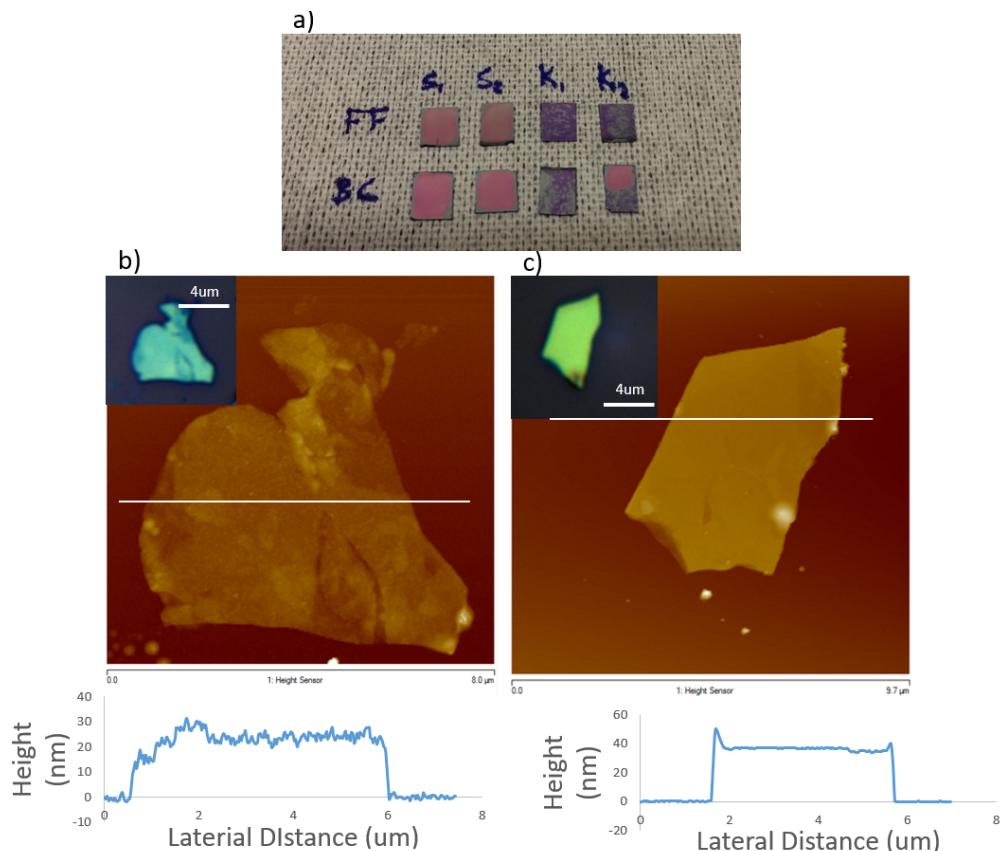


Figure 2.9. (a) Optical image of spin-coat comparison test sample. The left 4 substrates were exfoliated by the scotch tape while the right 4 were exfoliated by kapton tape. (b) AFM image (top), height profile (bottom), and optical micrograph (inset) of a scotch tape exfoliated As-GeH sample. (c) AFM image (top), height profile (bottom), and optical micrograph (inset) of a PDMS exfoliated Ga-GeH sample.

2.3 Optimized Cleaning Process

However, the PDMS-exfoliated substrates (**Figure 2.10a**) usually have some bright spots on the surface including the PDMS residues which cannot dissolve in acetone and isopropanol. Lithium phenylacetylide is expected to be capable of removing PDMS residues (**Figure 2.10b**). In this case, lithium phenylacetylide acts as a nucleophile while PDMS acts as electrophile (**Figure 2.11**). In PDMS, O is more electronegative than Si so O has a partial negative charge while Si bears a partial positive charge. In lithium phenylacetylide, the carbon-carbon triple bond grabs one electron from lithium so the $\text{C}\equiv\text{C}^-$ can attack the Si – O bond from PDMS and finally dissolve PDMS. Circles in figure 2.10a mark the bright spots which are absent in figure 2.10b

while the height profile shows that the flake surface was not etched after 90 min in lithium phenylacetylide, too. Therefore, lithium phenylacetylide can remove PDMS residues and is safe

to GeH flakes.

Chapter 3: Synthesis and Characterization of Germanane and its Derivatives

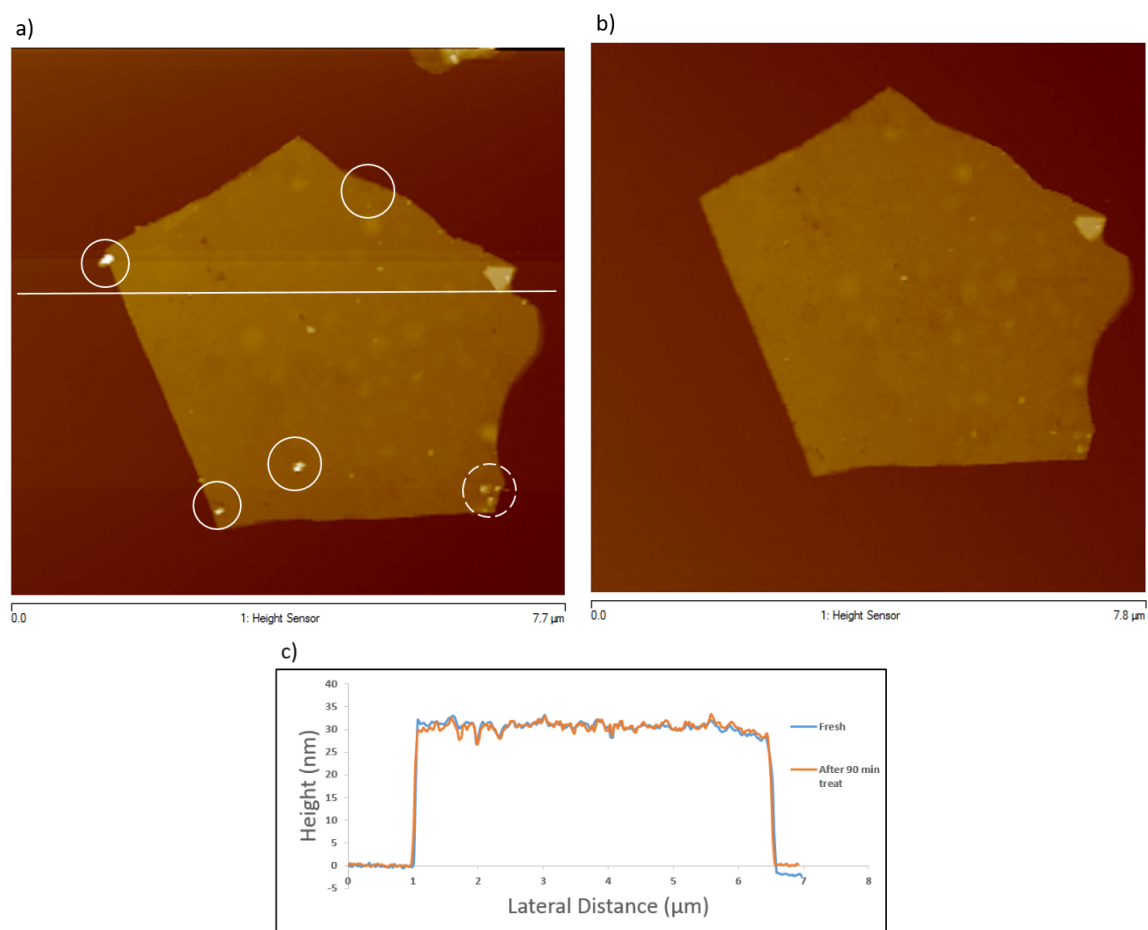


Figure 2.10. (a) Fresh exfoliated Ga-GeH flake. (b) The same flake after 90 min lithium phenylacetylide treatment. (c) Height profile of (a) and (b).

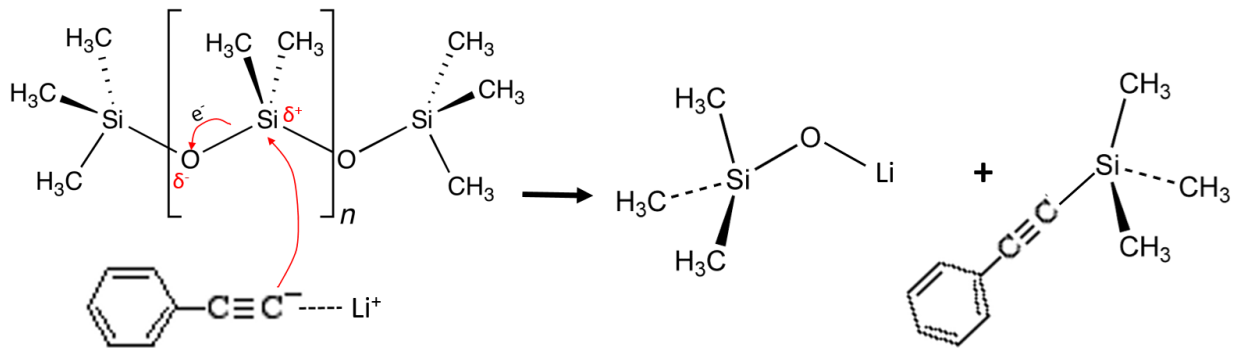


Figure 2.11. Schematic illustration of PDMS dissolving in lithium phenylacetylide.

Recently, Goldberger's group has developed gram-scale crystallites of hydrogen-terminated germanane. Generally, GeH is synthesized by the topotactic deintercalation of β -CaGe₂ in the concentrated HCl aqueous solution for one week and the whole reaction system is at -40°C (Figure 3.1). β -CaGe₂ crystals are prepared firstly by grinding Ca and GeH together at stoichiometric ratios and sealed in the quartz tube followed by annealing at 950°C and then cooling down to the room temperature in 2 ~ 10 days (Figure 3.1b). After one week in concentrated HCl solution, the product is rinsed by distilled water as well as methanol to get pure

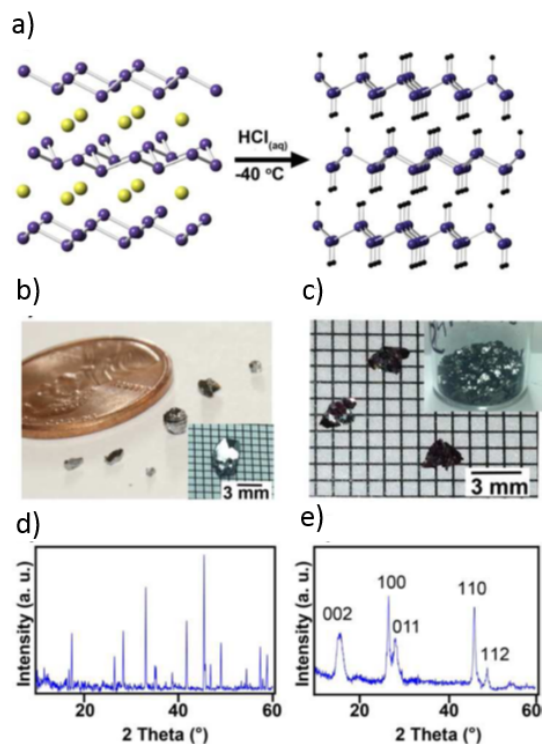


Figure 3.1 (a) Schematic illustration of the GeH preparation. (b) Optical image of β -CaGe₂ crystal. (c) Optical image of GeH crystal. (d) XRD diagram of (b). (e) XRD diagram of GeH.¹⁸

germanane (Figure 3.1 c). The purity of both β -CaGe₂ and GeH is demonstrated via X-ray diffraction (Figure 3.1de), respectively.¹⁷

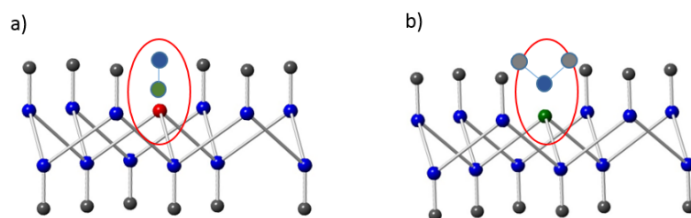


Figure 3.2. Schematic diagrams of (a) Ga-GeH and (b) As-GeH and p-GeH.

In order to modify the conductivity of GeH, we have developed three doped germanane: phosphorus-doped germanane (P-GeH), gallium-doped germanane (Ga-GeH) and arsenic-doped germanane (As-GeH). Ga-GeH (**Figure 3.2a**) is a p-type semiconductor material because its outer shell has one electron less than Ge. P-GeH and As-GeH (**Figure 3.2b**) are n-type

semiconductor materials because both P and As have one more electron on the outer shells than Ge. The syntheses of all the three doped GeH are quite similar to it of pure GeH. As for the synthesis of Ga-GeH, β -CaGe₂ is replaced by CaGeGa which shares a similar solid state synthesis process with β -CaGe₂. Then CaGeGa crystals would reaction with concentrated HCl solution at -40°C for one week to get GaGeH. As-GeH and P-GeH are prepared by the topotactic deintercalation of CaGeAs and GaGeP in the concentrated HCl at -40°C for one week, respectively. The purity of As-GeH and Ga-GeH have been demonstrated by X-ray diffraction spectroscopy (**Figure 3.3a**). In addition, XRD diagrams also prove that the crystal structure of As-GeH and Ga-GeH are similar to GeH. P-GeH is very similar to As-GeH so its crystal structure should be similar to pure germanane.

Fourier transform infrared spectroscopy (FTIR) (**Figure 3.3b**) and Raman spectroscopy

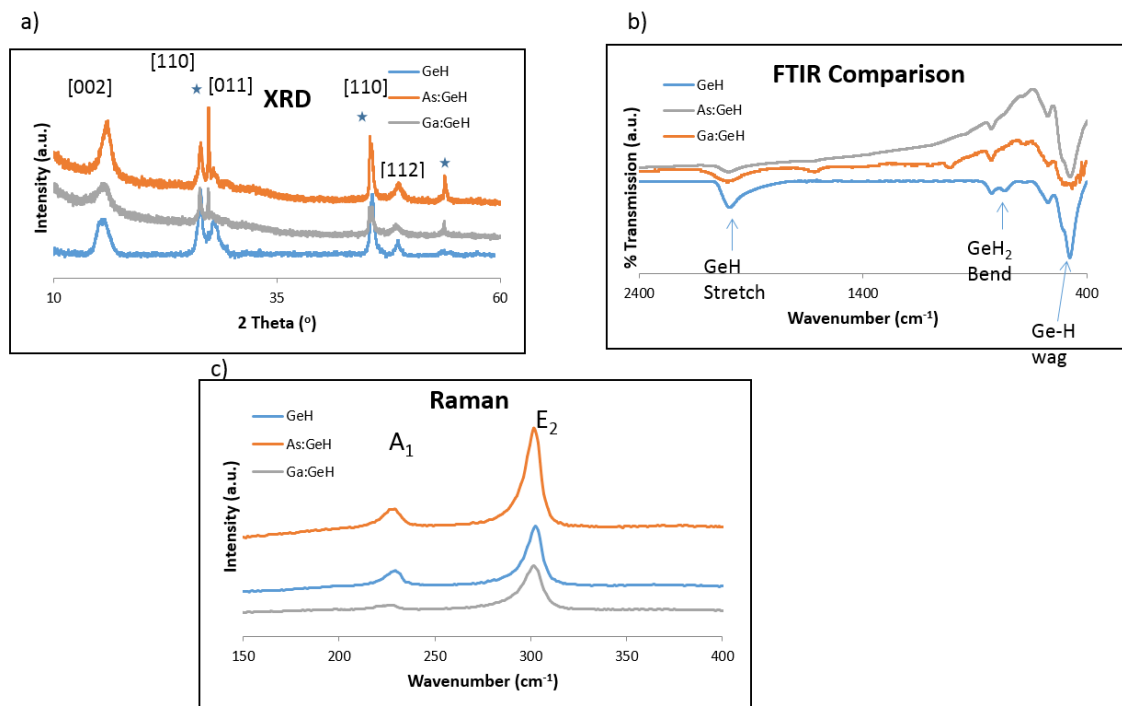


Figure 3.3. (a) XRD spectra (b) FTIR spectra and (c) Raman spectra of Ga-GeH, As-GeH and GeH.

(**Figure 3.3c**) were also applied to determine the crystal structure of Ga-GeH and As-GeH. In the transmission mode, Ga-GeH and As-GeH have Ge-H stretch peaks at $\sim 2000 \text{ cm}^{-1}$ and Ge-H wagging peaks at $\sim 476 \text{ cm}^{-1}$. In addition, a Ge-H₂ bending peak is also observed at $\sim 822 \text{ cm}^{-1}$ in both Ga-GeH and As-GeH. In Raman spectra, there are vibrational peaks at 230 nm (A₁ mode) and 303 nm (E₂ mode), respectively. Therefore, doping Ga and P do not change the crystal structure of GeH.

Chapter 4: Stability Studies

4.1 Air-Stability (XPS)

The previous work has proven that the hydrogen-terminated germanane materials can be oxidized slowly in the ambient atmosphere but the oxidization is bounded to the top layer (about

0.5 nm) while the bulk part is still resistant to the air.¹⁸ Sensors, transistors and transparent conducting electrodes are commonly exposed to the air and the air-stability of GeH promises its potential applications on these areas.

Doped GeH materials have a higher carrier concentration so the conductivity should be better than pure germanane. Therefore, we set a series of time-dependent XPS measurements to investigate the air-stability properties of doped GeH. In this case, As-GeH (Figure 4.1) and Ga-GeH (Figure 4.2) were analyzed. As for As-GeH, the sample was scanned immediately followed by being exposed to the ambient atmosphere and scanned after 1 day, 4 days and 8 days, respectively. After one day in the air, the 2p Ge⁺ peak at 1217.6 eV has a shoulder peak at 1220 nm which is Ge^{2+/3+} and the intensity of this shoulder peak is similar to the Ge⁺ peak after 8 days in the air (**Figure 4.1b**). In the 3d XPS spectra, the Ge⁺ peak at 29.9 eV also has a shoulder peak but the intensity of this shoulder peak is relatively weak after 8 days (**Figure 4.1a**). In the contrast, the 3d peak of As⁰ does not change after 8 days in the air.

The-time dependent XPS investigation of Ga-GeH is very similar to As-GeH. In the 2p XPS spectra, the Ge⁺ peak has an intensive shoulder peak after 8 days (**Figure 4.2b**). The 3d peak of Ge⁺ also has a weak shoulder peak after 8 days in the air while the 3d peak of Ga⁰ does not shift (**Figure 4.2a**). However, compared with the 3d Ge⁺ shoulder peak from As-GeH, the same shoulder of Ga-GeH is much less intense. In addition, the intensity 2p Ge^{2+/3+} peak is very similar to the 2p Ge⁺ peak after 8 days in the air in both As-GeH and Ga-GeH but after 5 months in the air, the Ge^{2+/3+} is still much less intense than the Ge⁺ peak in pure GeH (Figure 4.3). XPS is a sensitive method to analyze the oxidization state of elements on the surface, the intensity difference of a similar peak should be precise. In this case, our hypothesis is that the doped GeH

would be oxidized easier than the pure GeH; Ga-GeH is relatively more resistant to the air than As-GeH.

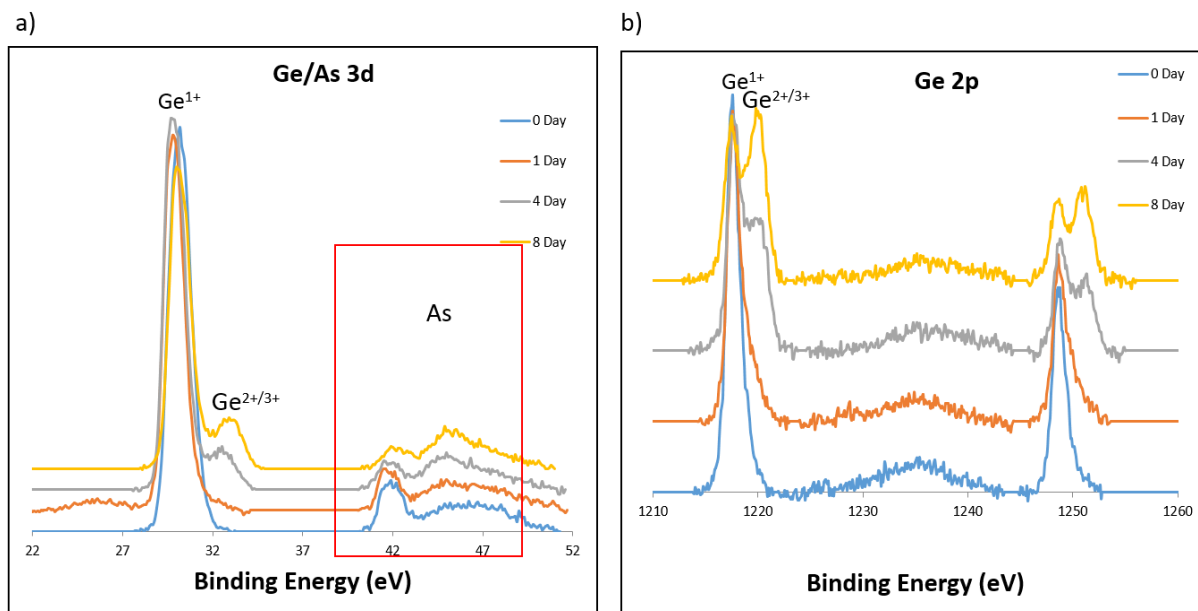


Figure 4.1. (a) 3d XPS spectra and (b) 2p XPS spectra of As-GeH.

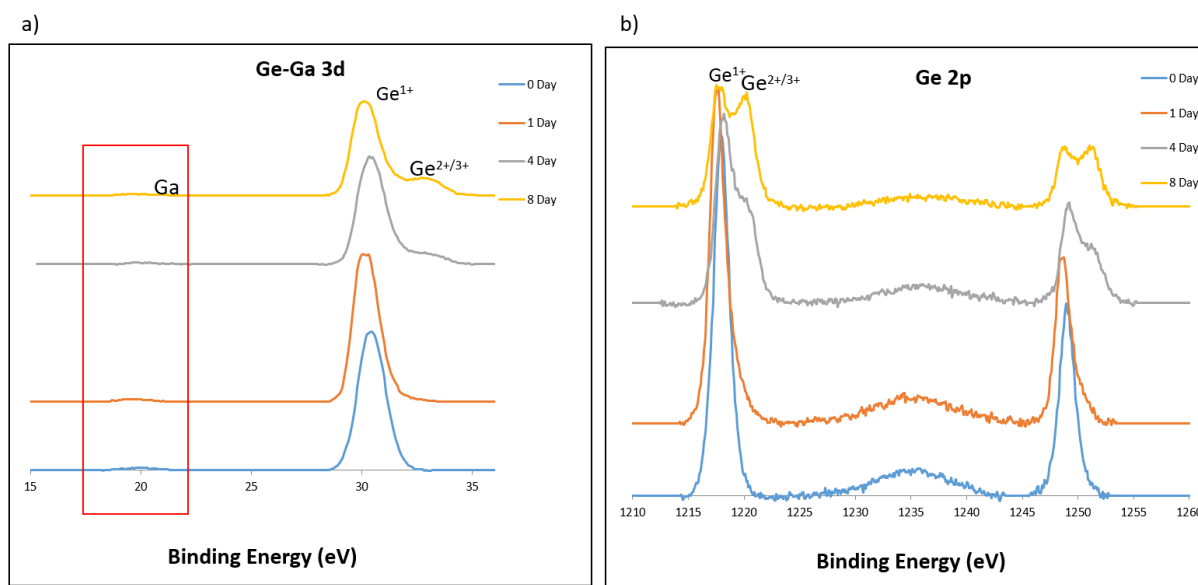


Figure 4.2. (a) 3d XPS spectra and (b) 2p XPS spectra of Ga-GeH.

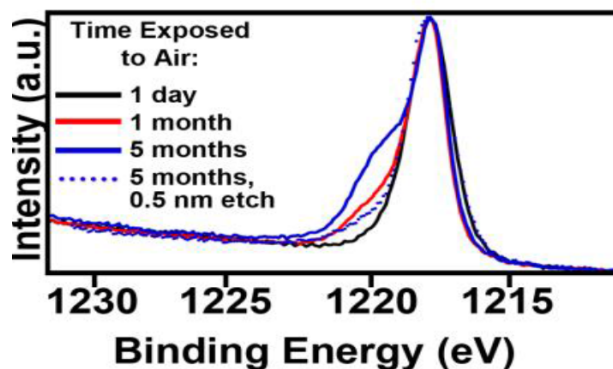


Figure 3.3. Time-dependent XPS spectra of GeH after exposure to the air for a period of time.¹⁸

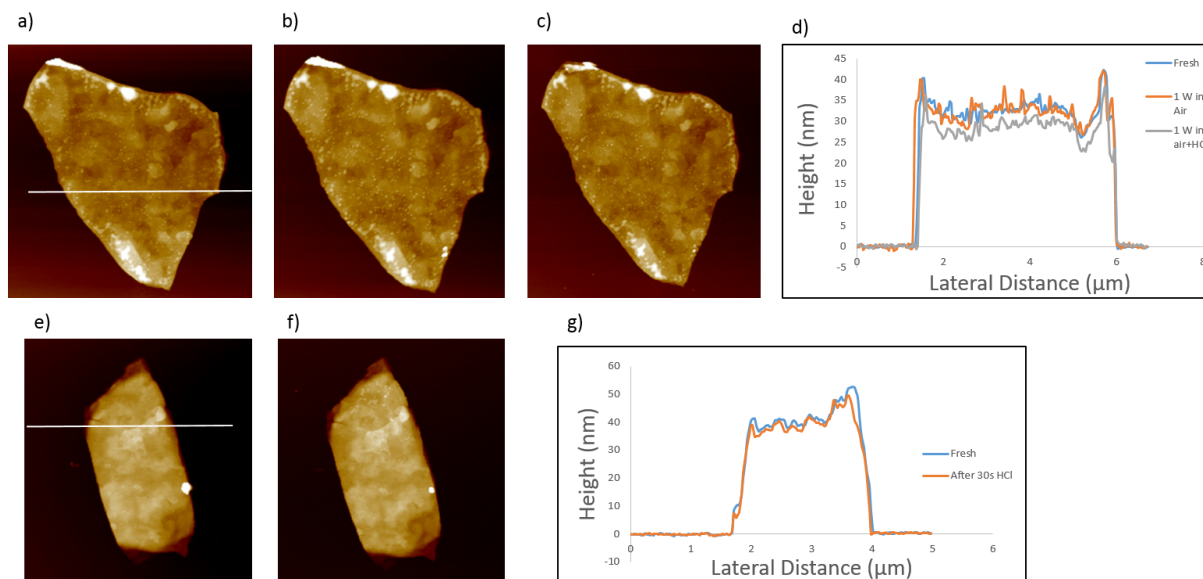


Figure 4.4. (a) AFM image of a fresh Ga-GeH flake. (b) AFM image of (a) after one week in air. (c) AFM image of (b) after 30 seconds 1 M HCl treat. (d) Height profile of (a), (b) and (c). (e) AFM of another fresh Ga-GeH flake. (f) AFM of (e) after 30 seconds in 1 M HCl. (g) Height profile of (e) and (f).

4.2 Air-Stability (AFM)

A time-dependent AFM study was placed to the air-stability studies of doped GeH. After one week exposure to the air (**Figure 4.4b**), there was no obvious changes on thickness and compared with the fresh flake (**Figure 4.4a**). After 30 seconds in 1 M HCl aqueous solution, this air-exposed Ga-GeH flake was etched by ~ 4 nm (**Figure 4.4c**). In contrast, the fresh GeH flake was etched little (~ 0.2 nm) after 30 seconds in 1 M HCl aqueous solution (**Figure 4.4f**). The only difference between an air-exposed flake and a fresh one is that the oxidizing period and XPS has

proved that GeH would be oxidized slowly in the air, thus proving that the HCl aqueous solution

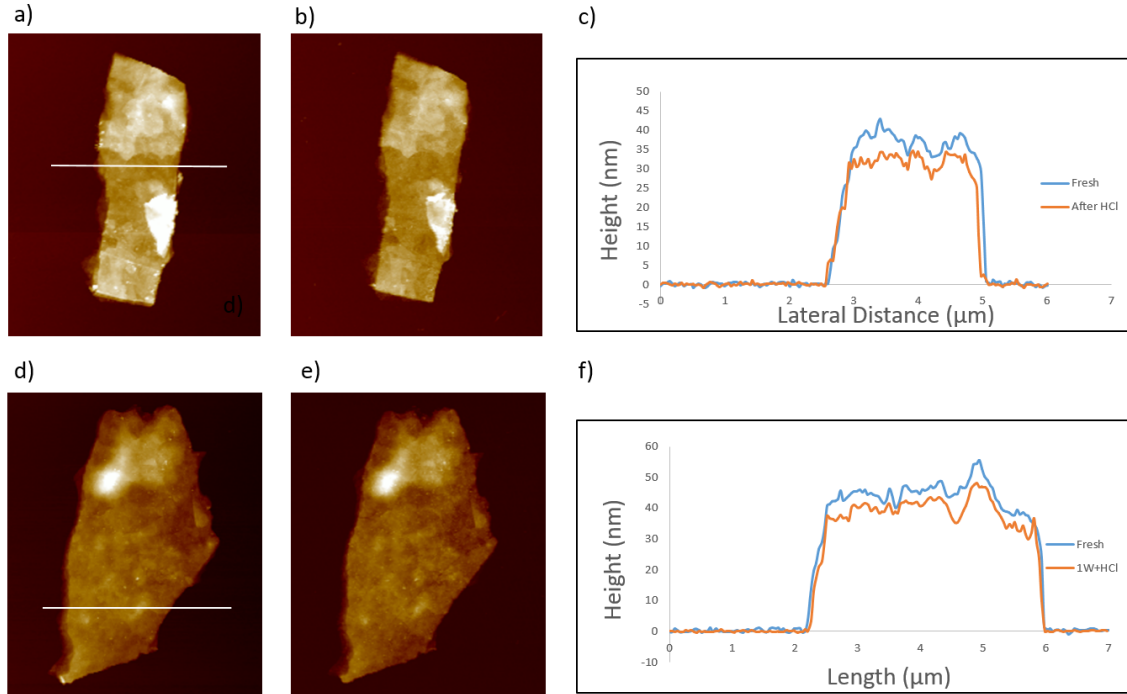


Figure 4.5. (a) AFM image of a fresh As-GeH flake. (b) AFM image of (a) after one week in air. (c) Height profile of (a) and (b). (d) AFM of another fresh As-GeH flake. (e) AFM of (d) after 30 seconds in 1 M HCl. (f) Height profile of (d) and (e).

can dissolve oxidized.

In addition, XPS data have proven that As-GeH and GeH can be oxidized. We did the same 30 second 1 M HCl solution test on As-GeH, P-GeH and GeH, respectively, as what we did on Ga-GeH. We kept one exfoliated As-GeH flake in the air for one week followed by a 30 second 1 M HCl solution test. AFM images show that the one-week-in-air As-GeH flake (**Figure 4.5b**) becomes darker and has holes/a rougher surface after the HCl treatment compared with the fresh image (**Figure 4.5a**). The fresh As-GeH flake (**Figure 4.5de**) shares similar changes on the surface with the oxidized one after the HCl treatment. The height profile of the oxidized flake (**Figure 4.5c**) shows that the flake was etched by ~ 5 nm after the HCl treatment while the etched thickness of the fresh flake was ~ 4 nm after HCl treatment (**Figure 4.5f**).

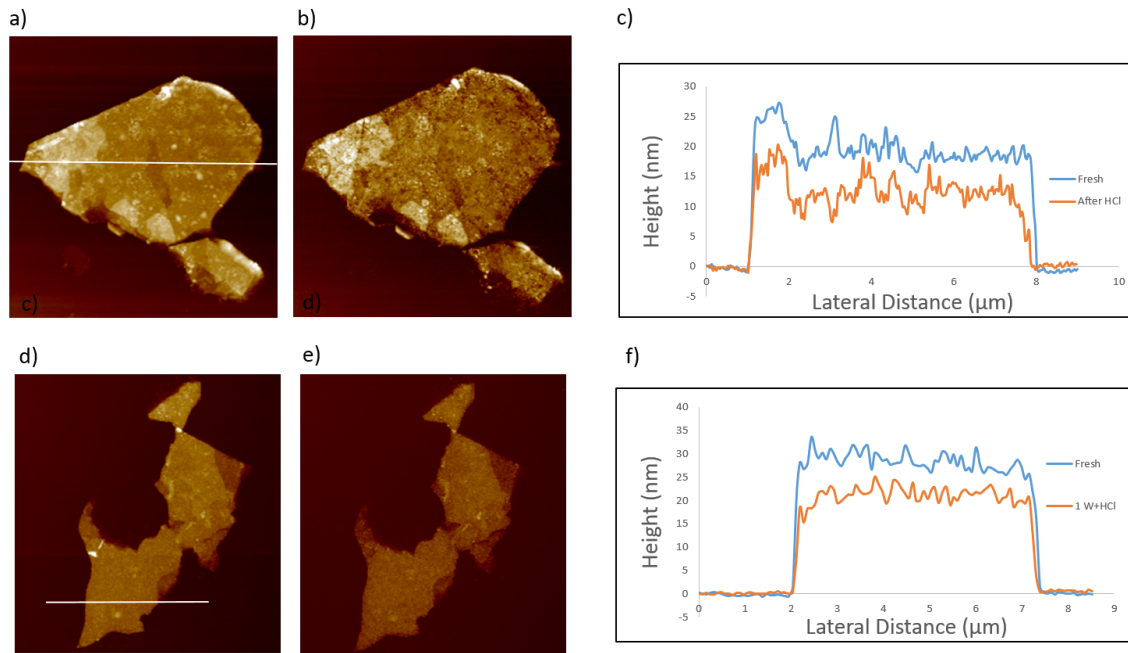


Figure 4.6. a) AFM image of a fresh P-GeH flake. (b) AFM image of (a) after one week in air. (c) Height profile of (a) and (b). (d) AFM of another fresh P-GeH flake. (e) AFM of (d) after 30 seconds in 1 M HCl. (f) Height profile of (d) and (e).

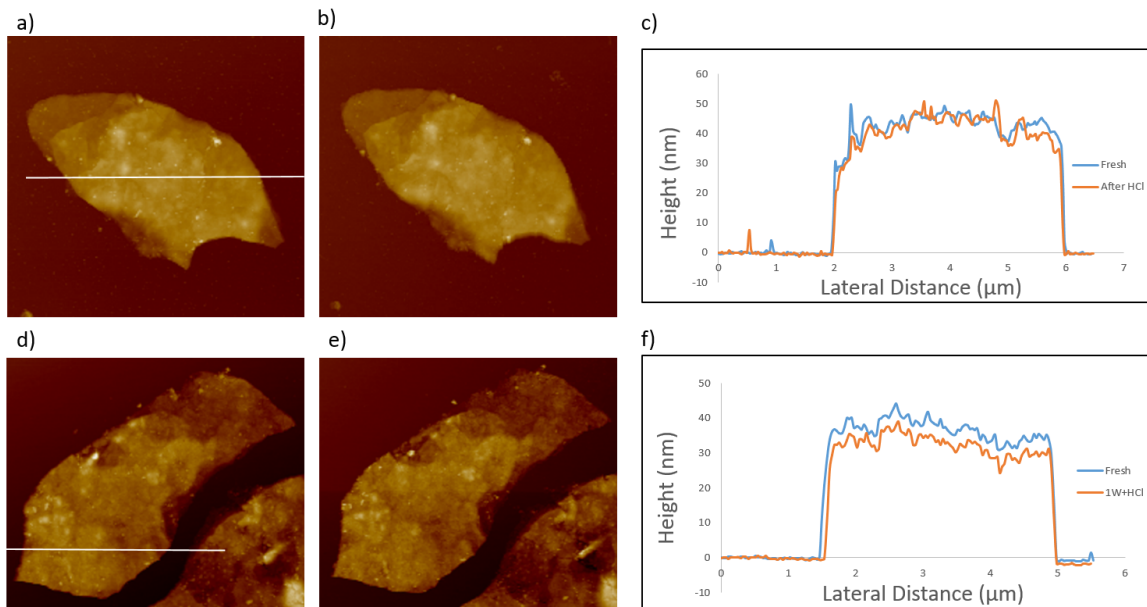


Figure 4.7. a) AFM image of a fresh GeH flake. (b) AFM image of (a) after one week in air. (c) Height profile of (a) and (b). (d) AFM of another fresh GeH flake. (e) AFM of (d) after 30 seconds in 1 M HCl. (f) Height profile of (d) and (e).

As for P-GeH, the one-week-air-exposure flake would be etched by 1 M HCl by ~ 7 nm in 30 seconds compared with ~ 6 nm etched thickness of a fresh P-GeH flake (**Figure 4.6**). Pure germanane is relatively stable: after one week in the ambient atmosphere, the flake would be

etched by ~ 4 nm (**Figure 4.7b**) after HCl treatment while the fresh one can only be etched by ~ 0.3 nm (**Figure 4.7e**) after HCl treatment. The etching effect on the air exposed flakes are similar while the etching rate on fresh flakes are variable from different materials. Therefore, the oxidizing rate can be determined based on the etching effect on fresh flakes so the four germanane materials have the following oxidizing rate order:

$$\text{P-GeH} > \text{As-GeH} > \text{Ga-GeH} > \text{GeH}.$$

4.3 HCl-Stability

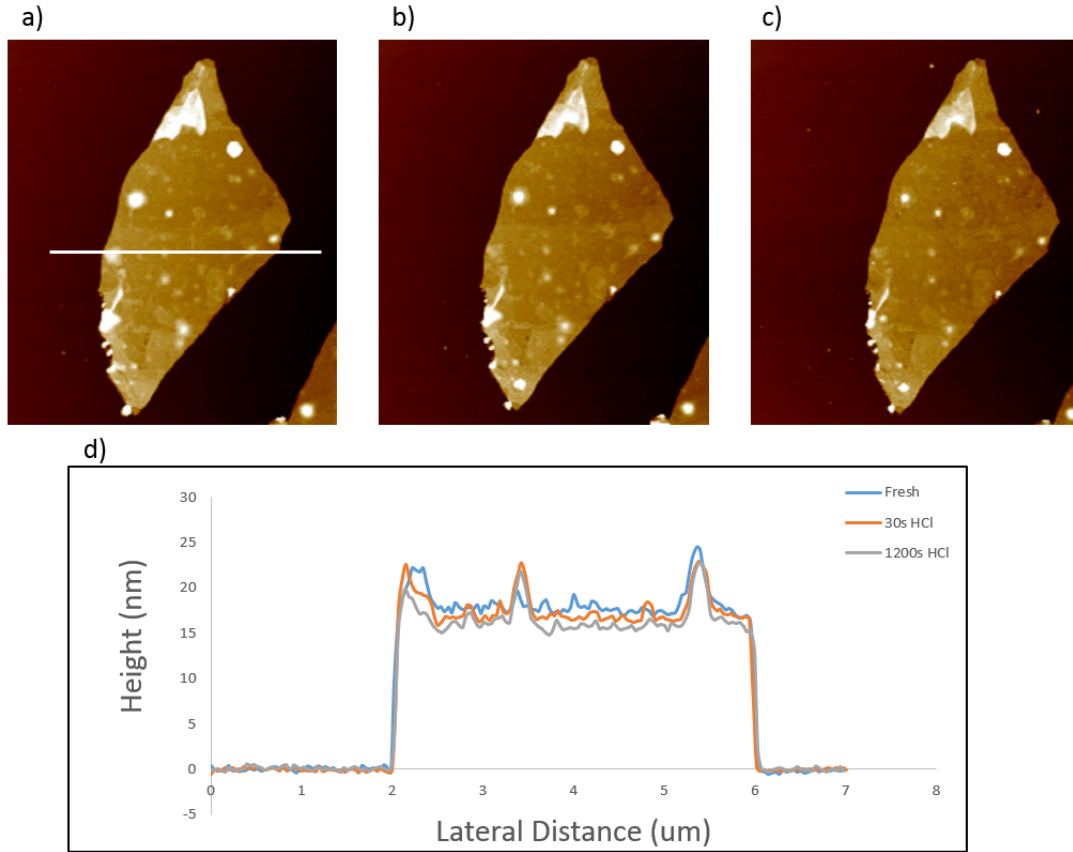


Figure 4.8. (a) AFM image of fresh-exfoliated Ga-GeH. (b) AFM image of (a) after 30 seconds 1 M HCl treatment. (c) AFM image of (b) after 1200 seconds 1 M HCl treatment. (d) Height profile of (a), (b) and (c).

As mentioned previously, GeH was prepared by the topotactic deintercalation of CaGe_2 in concentrated HCl aqueous solution at low temperature for at least one week. Another three doped GeH crystals were prepared in a similar process as GeH. In addition, all the 4 types of GeH would be oxidized in the ambient atmosphere and the oxidized layers can dissolve in 1 M HCl aqueous solution. Therefore we placed a 30-second-HCl-treatment versus 1200-second-HCl treatment test (**Figure 4.8**).

We place a 30-second-1-M-HCl-treatment on a fresh-exfoliated Ga-GeH flake just after scanning this flake under AFM followed by placing a 1200-second-1-M-HCl-treatment on the same flake and scanning under AFM again. Compared with the fresh AFM image (**Figure 4.8a**), the post 30-second-1-M-HCl-treatment flake (**Figure 4.8b**) is etched by ~ 0.8 nm. The flake is etched by ~ 1.0 nm after 1200-second-1-M-HCl-treatment (**Figure 4.8c**) compared with the flake after 30-second-HCl-treatment. Considering differences can rise from the interactions among the AFM tip, the multilayer sheet and the applied substrate, the etching effect on fresh flakes are independent on the time of the HCl treatment once the treatment period is longer than 30 seconds.¹⁹ Therefore, we hypothesis that the GeH materials are resistant to the HCl aqueous solution but the oxidized layers would be dissolved by the HCl solution.

Chapter 5: Further Work

2D materials have properties distinct from their parent materials because of the reduced dimensionality. The Group IV Graphane Analogues are an emerging class of 2D materials that show exceptional promise in a wide range of optical and electronic properties. Although we set a route of getting measureable GeH multilayers at this moment, they still have a bunch of potential applications such as batteries, p-n junctions and supercapacitors.¹⁸ We currently are measuring the electric properties of four types of germanane materials. The exfoliated flakes would be applied to make fabricating devices in the clean room and 4-probe measurement as well as 3-probe measurement would be placed on the fabricating devices. The 4-probe measurement is designed to eliminate the disturbance from the applied conducting materials and is capable to demonstrate the resistance of germanane materials individually. The 3-probe measurement is applied to measure the carrier-concentration-dependent conductivity, the mobility of carriers and identify the carrier (holes or electrons).

Generally, germanane materials are resistant to the air while the surface parts can still be oxidized. In addition, precise electric measurements require a clean surface to minimize unknown contributions. A 30 second UV-ozone plasma cleaning followed by 30 seconds 1 M HCl treatment is applied because the ozone plasma cleaning can remove most chemical residues and oxidizes flakes slightly compared with the oxygen plasma cleaning (**Figure 5**). Besides, we have developed doped GeH materials with doping concentration range 1% to 3% and in the soon future, we plan to develop doped GeH crystals with doping concentrations as high as possible to

make GeH 2D materials more practical because the conductance is proportional to the number of electron carriers.

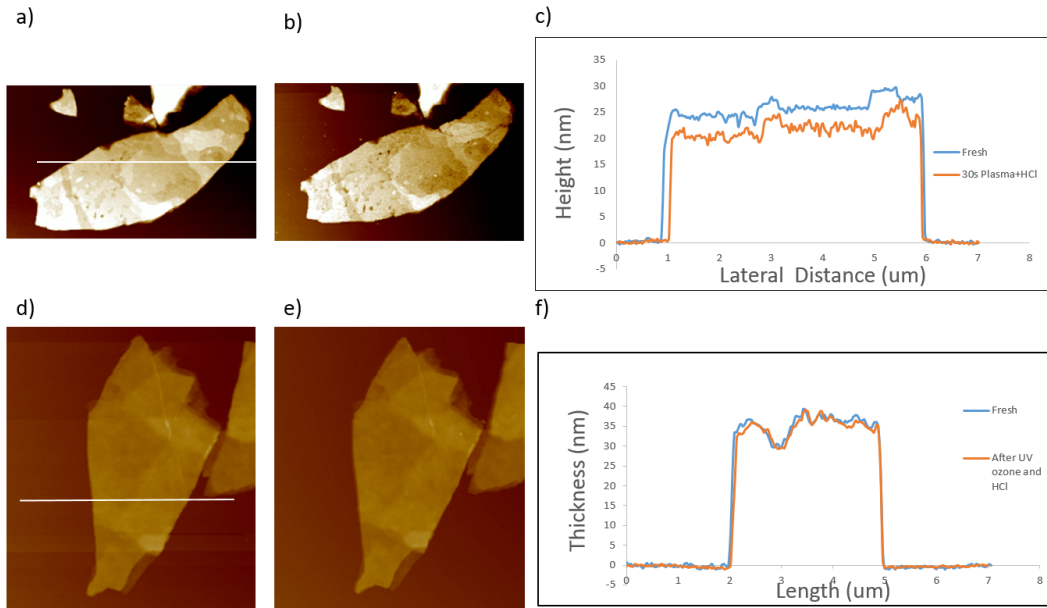


Figure 5. (a) AFM image of fresh Ga-GeH flake. (b) AFM of (a) after 30 second oxygen plasma followed by 30 seconds 1 M HCl treatment. (c) Height profile of (a) and (b). (d) AFM of fresh Ga-GeH flake. (e) AFM of (d) after 30 seconds UV-ozone plasma followed by 30 seconds 1 M HCl. (f) Height profile of (d) and (e).

Conclusion

In summary, we have synthesized gram-scale crystallites of gallium-doped, arsenic-doped, and phosphorus-doped hydrogen-terminated germanane and demonstrated all the three materials can be exfoliated into measureable multilayers on the SiO_2/Si substrates which would be used to make fabricating devices for the optical and electrical property studies. Besides, we have proven the cleaning effect of lithium phenylacetylide on the polydimethylsiloxane residues. We also characterized the oxidization-resistance of 4 types of exfoliated GeH which is an important prerequisite for practical applications and demonstrated that only the oxidized layers can be dissolved by HCl aqueous solution which essentially supports our synthesis procedure of GeH and its derivatives. Besides, the etching effect on different oxidized GeH flakes is quite similar: the etch height is 4~6 nm of all the four GeH materials although they have different oxidizing rate. In this case, we hypothesize that the pure GeH materials are resistant to the HCl aqueous solution while the oxidized layers are not; the oxidization is limited on the surface while the left flakes are resistant to the air. Thus, the stability of GeH and its three derivatives meets the prerequisite of potential applications.

References:

1. Novoselov, K. S.; Geim, A. K.; Morozov, S. V.; Jiang, D.; Katsnelson, M. I.; Grigorieva, I. V.; Dubonos, S. V.; Firsov, A. A. Two-Dimensional Gas of Massless Dirac Fermions in Graphene *Nature* **2005**, *438*, 197-200.
2. Novoselov, K. S.; Geim, A. K.; Morozov, S. V.; Jiang, D.; Zhang, Y.; Dubonos, S. V.; Grigorieva, I. V.; Firsov, A. A. Electric Field Effect in Atomically Thin Carbon Films *Science* **2004**, *306*, 666-69.
3. Fowler, J. D.; Allen, M. J.; Tung, V. C.; Yang, Y.; Kaner, R. B.; Weiller, B. H. Practical Chemical Sensors from Chemically Derived Graphene *ACS Nano* **2009**, *3*, 301-6.
4. Liang, Y.; Li, Y.; Wang, H.; Zhou, J.; Wang, J.; Regier, T.; Dai, H. Co₃O₄ Nanocrystals on Graphene as a Synergistic Catalyst for Oxygen Reduction Reaction *Nat. Mater.* **2011**, *10*, 780-86.
5. Williams, G.; Seger, B.; Kamat, P. V. TiO₂-Graphene Nanocomposites. UV-Assisted Photocatalytic Reduction of Graphene Oxide *ACS Nano* **2008**, *2*, 1487-91.
6. Lee, C.; Yan, H.; Brus, L. E.; Heinz, T. F.; Hone, J.; Ryu, S. Anomalous Lattice Vibrations of Single- and Few-Layer MoS₂ *ACS Nano* **2010**, *4*, 2695-700.
7. Mak, K. F.; Lee, C.; Hone, J.; Shan, J.; Heinz, T. F. Atomically Thin MoS₂: A New Direct-Gap Semiconductor *Phys. Rev. Lett.* **2010**, *105*, 136805.
8. Radisavljevic, B.; Radenovic, A.; Brivio, J.; Giacometti, V.; Kis, A. Single-layer MoS₂ Transistors *Nat. Nano.* **2011**, *6*, 147-50.
9. Elias, D. C.; Nair, R. R.; Mohiuddin, T. M. G.; Morozov, S. V.; Blake, P.; Halsall, M. P.; Ferrari, A. C.; Boukhvalov, D. W.; Katsnelson, M. I.; Geim, A. K.; Novoselov, K. S. Control of Graphene's Properties by Reversible Hydrogenation: Evidence for Graphane *Science* **2009**, *323*, 610-13.

10. Lomeda, J. R.; Doyle, C. D.; Kosynkin, D. V.; Hwang, W.-F.; Tour, J. M. Diazonium Functionalization of Surfactant-Wrapped Chemically Converted Graphene Sheets *J. Am. Chem. Soc.* **2008**, *130*, 16201-06.
11. Kagan, C. R.; Mitzi, D. B.; Dimitrakopoulos, C. D. Organic-Inorganic Hybrid Materials as Semiconducting Channels in Thin-Film Field-Effect Transistors. *Science*. **1999**, *286*, 945–947.
12. Huang, X.; Li, J.; Fu, H. The First Covalent Organic-Inorganic Networks of Hybrid Chalcogenides: Structures That May Lead to a New Type of Quantum Wells. *J. Am. Chem. Soc.* **2000**, *122*, 8789–8790.
13. Mitzi, D. B. Solution Processing of Chalcogenide Semiconductors via Dimensional Reduction. *Adv. Mater.* **2009**, *21*, 3141–3158.
14. Huang, X.; Roushan, M.; Emge, T. J.; Bi, W.; Thiagarajan, S.; Cheng, J.-H.; Yang, R.; Li, J. Flexible Hybrid Semiconductors with Low Thermal Conductivity: The Role of Organic Diamines. *Angew. Chem., Int. Ed.* **2009**, *48*, 7871–7874.
15. Becerril, H. A.; Mao, J.; Liu, Z.; Stoltenberg, R. M.; Bao, Z.; Chen, Y. Evaluation of Solution-Processed Reduced Graphene Oxide Films as Transparent Conductors *ACS Nano* **2008**, *2*, 463-70.
16. Vogg, G.; Brandt, M. S.; Stutzmann, M. Polygermyne_A. Prototype System for Layered Germanium Polymers. *Adv. Mater.* **2000**, *12*, 1278–1281.
17. Butler, S. Z.; Hollen, S. M.; Cao, L.; Cui, Y.; Gupta, J. A.; Gutierrez, H. R.; Heinz, T. F.; Hong, S.; Huang, J.; Ismach, A. F.; Johnston-Halperin, E.; Kuno, M.; Plashnitsa, V. V.; Robinson, R. D.; Ruoff, R. S.; Salahuddin, S.; Shan, J.; Shi, L.; Spencer, M. G.; Terrones,

- M.; Windl, W.; Goldberger, J. E. Progress, challenges, and opportunities in two-dimensional materials beyond graphene. *ACS nano*. **2013**, *7*, 2898-2926.
18. Bianco, E.; Butler, S.; Jiang, S. S.; Restrepo, O. D.; Windl, W.; Goldberger, J. E. Stability and Exfoliation of Germanane: A Germanium Graphane Analogue. *ACS Nano*. **2013**, *7*, 4414-21.
19. Nemes-Incze, P.; Osvath, Z.; Kamaras, K.; Biro, L. P. Anomalies in Thickness Measurements of Graphene and Few Layer Graphite Crystals by Tapping Mode Atomic Force Microscopy. *Carbon*. **2008**, *46*, 1435–1442.